HHS Public Access

Author manuscript

Bioconjug Chem. Author manuscript; available in PMC 2020 April 22.

Published in final edited form as:

Bioconjug Chem. 2020 February 19; 31(2): 248–259. doi:10.1021/acs.bioconjchem.9b00771.

Role of Albumin in Accumulation and Persistence of Tumor-Seeking Cyanine Dyes

Syed Muhammad Usama[†], **G. Kate Park**[‡], **Shinsuke Nomura**[‡], **Yoonji Baek**[‡], **Hak Soo Choi**[‡], **Kevin Burgess**[*,†]

[†]Department of Chemistry, Texas A & M University, College Station, Texas 77842, United States

[‡]Gordon Center for Medical Imaging, Department of Radiology, Massachusetts General Hospital and Harvard Medical School, Boston, Massachusetts 02114, United States

Abstract

Some heptamethine cyanine dyes accumulate in solid tumors *in vivo* and persist there for several days. The reasons why they accumulate and persist in tumors were incompletely defined, but explanations based on uptake into cancer cells via organic anion transporting polypeptides (OATPs) have been widely discussed. All cyanine-based "tumor-seeking dyes" have a chloride centrally placed on the heptamethine bridge (a "*meso*-chloride"). We were intrigued and perplexed by the correlation between this particular functional group and tumor uptake, so the following study was designed. It features four dyes (1-Cl, 1-Ph, 5-Cl, and 5-Ph) with complementary properties. Dye 1-Cl is otherwise known as MHI-148, and 1-Ph is a close analog wherein the *meso*-chloride has been replaced by a phenyl group. Data presented here shows that both 1-Cl and 1-Ph form noncovalent adducts with albumin, but only 1-Cl can form a covalent one. Both dyes 5-Cl and 5-Ph have a methylene (CH_2) unit replaced by a dimethylammonium functionality (N^+Me_2). Data presented here shows that both these dyes 5 do not form tight noncovalent adducts with albumin, and only 5-Cl can form a covalent one (though much more slowly than 1-Cl). In tissue culture experiments, uptake of dyes 1 is more impacted by the albumin in the media than by the pan-OATP uptake inhibitor (BSP) that has been used to connect uptake of tumor-seeking dyes *in vivo* with the OATPs. Uptake of 1-Cl in media containing fluorescein-labeled albumin gave a high degree of colocalization of intracellular fluorescence. No evidence was found for the involvement of OATPs in uptake of the dyes into cells in media containing albumin. In an *in vivo* tumor model, only the two dyes that can form albumin adducts (1-Cl and 5-Cl) gave intratumor fluorescence that persisted long enough to be clearly discerned over the background (~4 h); this fluorescence was still observed at 48 h. Tumors could be imaged with a higher contrast if 5-Cl is used instead of 1-Cl, because 5-Cl is cleared more rapidly from healthy tissues. Overall, the

[*]**Corresponding Author**: burgess@tamu.edu.

Author Contributions

This study was designed by K.B. who wrote the paper with contributions from S.M.U., G.K.P., and H.S.C. All the experimental work was performed by S.M.U., except the tumor models and imaging were from G.K.P. S.N. and Y.B. measured rates of excretion form the urine and blood plasma levels.

Supporting Information

The Supporting Information is available free of charge at PDF.

Synthesis scheme and procedures of 1, 5-Cl and -Ph, 2- Cl, and ICG and supporting figures (PDF)

The authors declare no competing financial interest.

evidence is consistent with *in vitro* and *in vivo* results and indicates that the two dyes in the test series that accumulate in tumors and persist there (1-Cl and 5-Cl, true tumor-seeking dyes) do so as covalent albumin adducts trapped in tumor tissue via uptake by some cancer cells and via the enhanced permeability and retention (EPR) effect.

Graphical Abstract

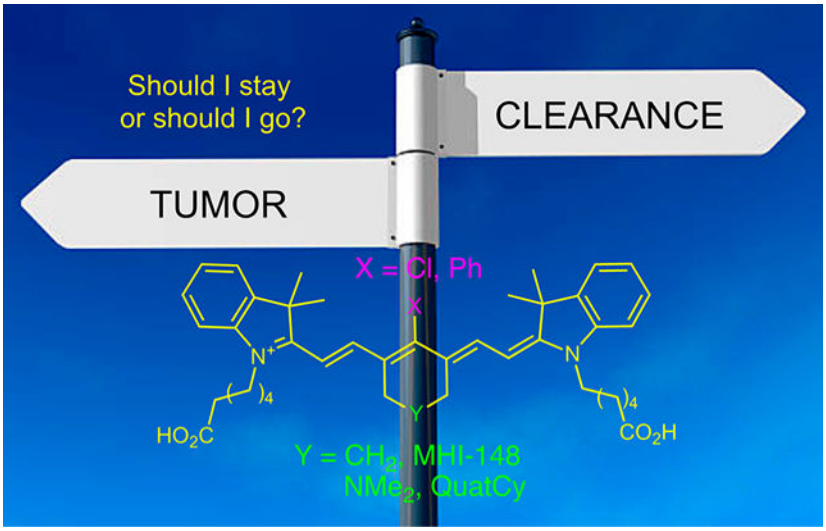

INTRODUCTION

Remarkably, some heptamethine cyanine dyes localize in any type of human solid tumor implanted into mice and their fluorescence persists there for several days. These cyanines have *clinical* potential for imaging applications. Moreover, their tumor-seeking properties can be exploited in drug conjugates for active targeting[1–10] where therapeutic effects may be enhanced due to retention in tumors. For both applications, formation of these dye conjugates provides a means to substantially alter the pharmacokinetics of small molecules that would not otherwise preferentially accumulate in tumors.

The importance of a fragment that actively targets *all* types of solid tumors should not be understated. A huge volume of research features mAbs[11,12] or small molecules[13,14] that bind cell surface receptors used in conjugation with cytotoxic species to increase therapeutic windows; those studies *only* target tumor cells expressing the corresponding receptors (e.g., folate or EGFR). “Tumor-seeking Cy7 dyes” (abbreviated to “Tumor seeking dyes” here), however, seem to target all solid tumor types, and could be particularly useful to address tumor heterogeneity[15] in individual patients, or in patient groups for which tumor-variations are ill-defined.

Tumor-seeking Cy7 dyes discovered so far all have a *meso*- chloride and a cyclohexenyl skeleton. For instance, fluorophore 1-Cl localizes in many different types of cancer lines and in solid tumors (e.g., prostate,[16] gastric,[17] kidney,[18]) but not in normal cells and tissue.[19–23] Cyanine 2-Cl is similar to 1-Cl except the *N*-substituents are one methylene group shorter and terminated with sulfonic acid groups. Like 1-Cl, the disulfonic acid 2-Cl selectively

localizes in tumors over healthy tissue,[19] *e.g.*, in hepatocytes,[9] kidney,[18] lung,[24] and intracranial human glioblastoma cells (U87).[8] Cyanine 3-Cl, is a hybrid of 1-Cl and 2-Cl with one sulfonic and one carboxylic acid. Fluorophore 3-Cl accumulates in solid tumors (*e.g.*, hepatocytes,[25] glioblastoma,[8] Burkitt Lymphoma,[10] breast cancer[6]). Cyanine 4-Cl has two propyl groups on indoles and has been reported to localize in lung and breast cancer[20] and stem cells.[26]

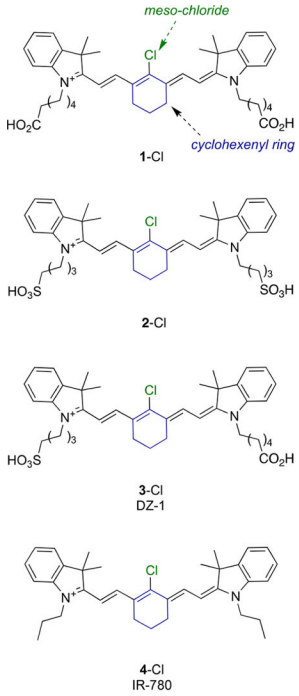

Several publications,[3,5,10,16–19,26–33] including one of ours,[34] have stated or implied preferential uptake of tumor seeking dyes like 1−4-Cl is mediated by organic anion transporting polypeptides (OATPs). This assertion is reasonable because hypoxia triggers activation of HIF1*α*, which promotes OATPs expression.[17,30] Further, OATPs are promiscuous; they influx organic anions including bile salts, steroids, bilirubin, and thyroid hormones and can take up unnatural organic molecules. OATPs do not efflux the same substrates, but instead bicarbonate is excreted to balance the charge; thus, molecules imported via OATPs are not necessarily pumped out the same way.

Contrary to the arguments implicating OATPs in uptake of tumor seeking dyes, in our minds the hypothesis is unproven, and it does not explain the structural feature that all these fluorophores share: a *meso*-chloride on a cyclohexenyl group. To the best of our knowledge, there is nothing in the literature to connect OATP-mediated transport with this functionality.

Recently, we discovered[35] that the *meso*-chloride of 1-Cl is displaced by *S*-nucleophiles under physiological conditions, including the free Cys residue in serum albumins (Cys^{34} in human serum albumin, HSA). Thus, in serum, where there is an extremely high concentration of albumin (around 35−50 g/L or 0.53−0.73 mM in humans),[36] 1-Cl may form a covalent adduct with a half-life of just over 30 min.[34] Similar data on the reaction of 1-Cl

with nucleophiles, including albumin, was simultaneously collected by Conovas et al. in an independent study.[37]

This manuscript explores the evidence commonly presented for involvement of OATPs in uptake of tumor seeking dyes, and rationalizes the two defining characteristics of those dyes,i.e., why they accumulate in tumors, and why they persist there.

RESULTS AND DISCUSSION

Compounds Considered.

Four key compounds in this study are 1-Cl, 1-Ph, 5-Cl, and 5-Ph. As mentioned above, 1-Cl reacts relatively rapidly under physiological conditions with the free Cys[34] thiol of albumin via displacement of the *meso*- chloride.[34,35] Reaction of 5-Cl (QuatCy)[38] with albumin is much slower under physiological conditions, but it will eventually form an analogous covalent adduct.[39] This difference is related to the extra positive charge on the QuatCy core (5) relative to framework 1 which impacts the electrostatic affinity of the two dyes toward {protein-based} nucleophiles, their water solubilities, logP (reflecting partitioning of ions) and logD (partitioning of all neutral species and ions) values.[38]

Derivatives of 1 wherein the *meso*-Cl is replaced by a phenyl group, i.e., 1-Ph and 5-Ph, are excellent controls because they have no chloride to be displaced by nucleophiles. They cannot form the same type of albumin adduct that 1-Cl and 5-Cl do, but are otherwise physiochemically similar.

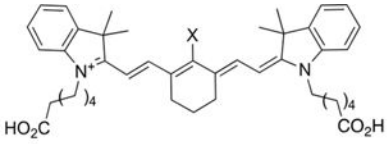

1

X = Cl, MHI-148, **1**-Cl, *reacts quickly with albumin*, logP= 6.57, logD= 3.82
= Ph, **1**-Ph, *cannot react with albumin*, 7.85, 5.09

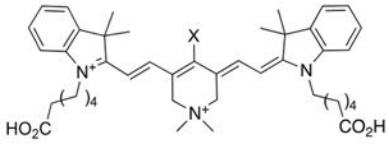

5

X = Cl, QuatCy, **5**-Cl, *reacts slowly with albumin*,1.10, 2.64
= Ph, **5**-Ph, *cannot react with albumin*, 2.38, 3.92

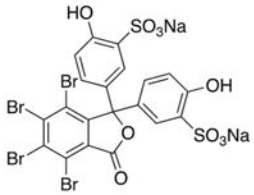

BSP

bromosulphthalein, or phenoltetrabromophthalein sodium sulphonate

Evidence Cited for Involvement OATPs: BSP Blocks Cellular Uptake in SFM.

Bromosulfophthalein (BSP) is a pan-OATP inhibitor,[40] and its effects on uptake of tumor-seeking dyes into cancer cells is uniformly cited as evidence for involvement of that receptor type. Thus, the following set of experiments has become standard when testing tumor-seeking near-IR dyes in tissue culture.[3,5,10,16−19,26−30,41] Incubation of the fluorophore with the cells *in serum free media* (SFM; i.e., containing 0% FBS) reveals a baseline level of uptake (Figure S1a for 1-Cl), but treatment with BSP *lowers* uptake, consistent with OATP inhibition. Conversely, pretreatment of the cells with DMOG, a small molecule that induces hypoxia,[17,30] promotes OATP expression which *enhances* uptake. Hypoxia has been reported to promote expression of OATPs,[8] so enhanced uptake into hypoxic cancer cells (in the absence of BSP) is consistent with involvement of OATPs.

Data collected for 1-Ph under the standard conditions outlined above (Figure 1) are not materially distinguishable from that accumulated in our lab for 1-Cl (Figure S1). Baseline uptake of 1-Ph (Figure 1a) was suppressed by BSP (Figure 1b), and enhanced under hypoxic conditions (Figure 1c). Thus, comparison of these observations with the corresponding data for 1-Cl (Figure S1) and 1-Ph (Figure 1) shows that *meso*-Cl substitution (only possible for 1-Cl, and not possible for 1-Ph) does *not* impact uptake in SFM.

Human MDA-MB-231 triple negative breast cancer cells were selected as a model line because they are derived from an aggressive metastatic tumor. However, HepG2 liver cancer cells were also tested to check generality throughout this study (Figures S16 and S17). HepG2 cells are particularly appropriate because BSP has special relevance to the liver (this is explained in depth later); hence, cells derived from liver-cancer were more likely to behave differently than many others. However, it emerged that there appears to be nothing unique about MDA-MB-231 cells that is relevant to the observations described below.

Effects of Albumin Outweigh Those of BSP in SFM.

Tissue culture experiments *in serum-containing media* (10% FBS used here), are *not* the same (Figure 2) as for those without serum (Figure 1). Without serum, quantitated levels (Figure 2e) show, as expected, uptake of 1-Cl and 1-Ph was significantly (40−50%) decreased by BSP. Uptake of 1-Cl in SFM under these conditions is marginally less than for 1-Ph, but the difference is small. However, serum had a greater negative impact on uptake of 1-Cl and of 1-Ph than BSP, i.e., uptake of 1-Cl and 1-Ph is suppressed in serum-containing media, even without added BSP.

Unexpectedly, uptake of the QuatCy derivatives 5-Cl and 5-Ph were enhanced by BSP in SFM (*note*: the degree of uptake was low anyway with respect to 1-Cl and 1-Ph (Figure S3), so differences in the measurements are less accurate than others in these experiments). Moreover, uptake of both QuatCy derivatives 5-Cl and 5-Ph were unaffected by serum, and only marginally depressed by BSP in serum (Figure S2).

The following experiment was performed to test whether albumin, the predominant protein in serum,[42−44] was the key component that caused the differences outlined above. Figures S12 and S13 shows uptake of all four featured compounds (1-Cl, 1-Ph, 5-Cl, and 5-Cl) when

BSA was added to SFM was almost identical to those in serum, supporting the assertion that albumin is indeed the key component.

Previous work[34,35] had already established that 1-Cl *covalently* binds albumin under physiological conditions, and that reaction is *not* instantaneous, so UV and fluorescence spectroscopies were used to probe the short-term effects of albumin and serum on this dye. Combinations of 1-Cl with HSA and of 1-Cl with serum (i.e., 10% FBS in DMEM buffer) both gave an *instant* red shift in the UV (and fluorescence). That shift was almost identical for 1-Cl combined with HSA, or with DMEM containing 10% FBS (Figures 3a and S4a). UV spectra of 1-Ph with HSA, and with serum, showed the same instantaneous absorption maxima red-shifts, attributed to *noncovalent* binding. On the basis of these observations, we conclude the instantaneous reaction of 1-Cl and 1-Ph in serum is to form a *non*-covalent adduct with albumin.

Figure 3 shows UV absorbance data for 1-Cl (a) and 1-Ph(b) in PBS with 50 equiv of HSA incubated for 0−5 h at 37 °C. At the first data point, 0.05 h, the absorbance maximum for the mixture featuring 1-Cl was completely red-shifted to 805 nm. After 5 h, a new UV spectrum formed corresponding to a species with an intermediate absorption maximum at 791 nm. Instantaneous red-shift from 780 to 805 nm, followed by a slower blue-shift to 791 nm, can be explained in the following way. Albumin rapidly forms a noncovalent adduct with MHI-148, 1-Cl, followed by slower transformation into a Cys^{34}-bound covalent adduct, consistent with the data we reported previously,[34,35] and the work of Canovas et al.[37] Support for this assertion comes from the corresponding experiment with the *meso*-blocked dye 1-Ph (Figure 3). For 1-Ph, Figure 3a shows addition of albumin led to instantaneous formation to a new UV spectrum with a red-shifted absorption maximum, which is invariant over 5 h, the time span of the experiment. Thus, 1-Ph with albumin forms only the noncovalent adduct; no covalent adduct was formed because there is no possibility of chloride displacement.

Experiments were performed to establish if the rest of the dyes in the series 1−5 also formed noncovalent adducts. Data for 2-Cl (IR-783) and ICG (both dyes with two sulfonate chains) show the same red-shifted absorbance maxima (with decreased absorbance) when mixed with albumin (Figures S14 and S15); thus, they both appear to form noncovalent adducts (prior literature exists on interaction of albumin with ICG,[45] and it is consistent). Incidentally, FACS experiments indicated import of 2-Cl and ICG into MDA-MB-231 breast cancer cells in SFM (suppressed by serum, BSP, and BSA (Figures S14b, c and S15b, c); this also parallels the data for 1-Cl. Absorption maxima of dyes 3-Cl and 4-Cl were known to be red-shifted in the presence of albumin,[25,46] implying noncovalent complexation. Behavior of the QuatCy derivatives 5-Cl and 5-Ph with albumin are markedly different from 1-Cl−4-Cl. Absorption maxima wavelengths and intensities of 5-Cl and 5-Ph were unperturbed on combination with albumin, hence neither forms a noncovalent adduct (data not shown).

Covalent bond formation of dyes 1-Cl−4-Cl was supported via HPLC analyses, and previous work by our group[34,35] and by Conovas et al.[37] The current study (Figure S11) showed that relative rates for the formation of covalent adducts were (at 37 °C with 2 equiv of HSA): 4-

Cl (IR780; $t_{1/2}$ 2 min) ≫ 1-Cl (6 h) > 3-Cl (24 h) > 2-Cl (72 h), and formation of an adduct from 5-Cl only proceeded to ~30% after 72 h under these conditions (data not shown). *In vivo* we expect the dyes to convert to covalent adducts more rapidly due to the high concentration of albumin in serum.[47]

BSP Cannot Displace MHI-Derivatives 1 from Their Noncovalent Complexes with Albumin.

The "standard uptake experiments" in SFM outlined above, that supposedly implicate OATP receptors, feature an interplay of the dye, BSP, and albumin, not just the dye and albumin. Consequently, UV and fluorescence spectroscopies were used to ascertain how BSP might impact interactions of the dyes with albumin.

BSP has such a high affinity for albumin that, according to one estimate,[48] more than 99% is bound to it after iv injection. According to another report, equimolar concentrations of BSP and albumin afforded less than 0.1% of unbound BSP.[49] Consequently, experiments were performed to ascertain if albumin-bound BSP could be displaced by 1-Cl. Thus, HSA and increasing concentrations of BSP (up to 50 equiv) were mixed, then 1-Cl was added (Figure S6c); no difference in absorbance maxima relative to the noncovalent dye•albumin complex was observed. This experiment was repeated with the opposite order of addition (Figure S6d, i.e., HSA and 1-Cl were mixed, then up to 50 equiv of BSP was added), but the outcome was essentially the same. In both experiments, the only significant impact of BSP on the mixture of HSA and 1-Cl was that the UV absorbance intensity was somewhat reduced, implying some interaction of BSP with the noncovalent albumin•1-Cl complex that does *not* replace the dye. Fluorescence spectra were also recorded, and similar shifts were observed (Figure S7). These data do not prove the binding of the dye to albumin is stronger than albumin•BSP, because BSP binds multiple binding sites on albumin,[50] but they do prove 1-Cl is not displaced from albumin by BSP. In another control experiment, BSP was shown not to influence the emission wavelength maxima of 1-Cl (though its fluorescence intensity was decreased by ~30% presumably due to a quenching effect; Figure S7b).

The experiments described above to probe interactions of albumin, BSP, and 1-Cl were performed over ~30 min after mixing so that very little *covalent* adduct 1-HSA forms. There was an unlikely possibility that both 1-Cl and BSP bound to albumin have such extremely slow k_{off} rates that dissociation of either species could not be forced by introducing the other into solution. To test for this, similar experiments were performed using a derivative that cannot form the covalent adduct, 1-Ph, over 5 h; the outcome was essentially the same (Figure S8) indicating extremely slow k_{off} rates are *not* clouding interpretation of the UV data.

Figure 3c shows an overall summary of the most important UV experiments described above, but some other, less important, observations were also made. BSP had no impact on the absorption maximum of 5-Cl mixed with albumin, consistent with the lack of formation of a noncovalent adduct (Figure S9). Warfarin, ibuprofen, and digoxin bind three different sites on albumin,[51,52] so these were coincubated with 1-Cl to attempt to identify the HSA binding pocket that 1-Cl occupies in the noncovalent complex (Figure S10). Ibuprofen had the greatest effect on the fluorescence spectra of 1-Cl mixed with BSA, but throughout, the perturbations were modest, hence these experiments were inconclusive.

Import into Hep2G Liver Cancer Cells.

Uptake of 1-Cl, 1-Ph, 5-Cl, and 5-Ph into HepG2 liver cancer cells were explored to test if there was something particular to MDA-MB-231 breast cancer cells. The data accumulated for these experiments (Figures S16 and 17) followed the same trends as identified above.

MHI-148 and Albumin-FITC in Media Are Imported into Cells and Colocalize.

In a key confocal microscopy experiment, 1-Cl and fluorescein-labeled BSA (FITC-BSA; noncovalent adduct) incubated with MBA-MD-231 cells colocalized (Figure 4a; Pearson coefficient 0.65) showing the noncovalent adduct is influxed and does not dissociate significantly in the cells. Predictably, images of cellular uptake, performed with 1-BSA-FITC (covalent adduct), are similar (Figure 4b; Pearson coefficient 0.54). When 1-Cl was preincubated with Cys^{34}-*blocked* BSA, this gave the same result (Figure 4c; Pearson coefficient 0.56), and 1-Ph and BSA-FITC also colocalized (Figure 4d; Pearson coefficient 0.63). Thus, 1-Cl is imported as a noncovalent complex that persists in cells.

Overall Conclusions from Cell Data Alone.

The hypothesis that uptake of tumor seeking dyes is mediated primarily by OATPs is not supported by the evidence accumulated above for media containing albumin. At a maximum, OATPs may be prevalent in SFM, but in serum (and in SFM plus albumin) they are not. The concentration of albumin in the blood is such that cellular experiments with cancer cells in SFM are not particularly relevant to *in vivo* uptake into tumors.

It was clear from the data discussed above that *in vivo* experiments were critical to establish the mode of uptake. If, contrary to the cell data, OATPs *were* dominant, then 1-Cl and 1-Ph, which behaved the same in SFM, should have similar accumulation and persistence characteristics *in vivo*. However, if covalent albumin binding was more important to tumor uptake and persistence *in vivo*, then the experiments with cancer cells outlined above would lead to the following predictions. In the short term, both 1-Cl and 1-Ph would be expected to permeate tumor tissue (since both are uptake in cancer cells in the presence of albumin). However, 1-Ph should be cleared quickly like most small molecules, whereas 1-Cl converted to 1-albumin adopted accumulation and persistence properties similar to albumin.

The key *in vivo* experiments described in the next section build upon some prior work that is summarized here. It was known that 1-Cl accumulates in solid tumors but also to a significant extent in the liver and kidneys,[3,5] this accumulation had never been compared with that of an analog that cannot form covalent adducts with albumin (e.g., 1-Ph). Our prior work had shown that the QuatCy derivative 5-Cl was cleared more quickly from healthy mice than 1-Cl.[38] We also had shown[38] that 5-Cl accumulated a murine tumor (pancreatic model) and was retained there for extended periods. However, the relative behavior of 5-Ph (blocked from covalent albumin adduct formation) was also an unknown.

In Vivo Clearance and Tumor Accumulation of Cyanines 1 and 5.

In vivo tumor accumulation of 1-Cl, 1-Ph, 5-Cl, and 5-Ph, and persistence of each dye for up to 48 h (Figure 5a) were compared in mice with subcutaneous triple negative breast tumors (E0771). This triple negative breast cancer tumor model was chosen to probe the

characteristics of the dyes in an orthotopic system, i.e. not involving immune compromised mice. Mice were intravenously injected with each fluorophore and imaged at 0.5, 1, 2, 4, 24, and 48 h post-injection. Tumor-to-background ratios (TBRs) were calculated by measuring the fluorescence intensity of the tumor against the nearby healthy tissue signal (background; Figure 5b).

meso-Phenyl derivatives of MHI148 (1-Ph) and QuatCy (5-Ph) had poor preferential tumor accumulation and no significant persistence (Figure 5a); hence, TBRs in these experiments did not deviate significantly from unity, i.e. there was little contrast between the tumor and the background. Conversely, 1-Cl and 5-Cl displayed high tumor accumulation and prolonged retention, where the maximum TBR was 3.5 and 10, respectively (48 h post-injection; Figure 5b). Accumulation of 1-Cl and 5-Cl into the tumor and background tissues was rapid, but 5-Cl cleared faster from the healthy tissue, giving comparatively high TBR values for each time point at which the tumor could be discerned (Figure 5a and b); high contrast was observed 4 h post-injection of 5-Cl, while 48 h was needed for 1-Cl. For intraoperative tumor resection, clearance from the nontarget organs is as important as dye accumulation and retention in target tissue. Thus, 5-Cl outperformed 1-Cl as a tumor-targeted contrast agent on this basis.

At 48 h post-injection, tumors and organs were resected from the body (Figure 6) so that relative biodistributions of the fluorophore could be measured. *meso*-Phenyl dyes (1-Ph and 5-Ph) were almost completely cleared from the body, but the *meso*-chloride dyes (1-Cl and 5-Cl) persisted (Figure S17). Pharmacokinetics was performed exclusively on 1-Cl and 5-Cl, because they alone in the series were retained in the tumors.

Biodistribution and clearance of 1-Cl and 5-Cl were compared in healthy CD-1 mice. QuatCy 5-Cl showed both renal and hepatic clearance, while 1-Cl was predominantly cleared via the liver. QuatCy, 5-Cl, was detected in the gastrointestinal tract from 1 h post-injection, indicating fast excretion from liver and bile duct, while 1-Cl still gave a signal in the liver and duodenum even after 4 h post-injection. Fluorescence measurements were used to monitor the compounds in the blood and urinary excretion for up to 5 h. Insignificant urinary excretion was observed for 1-Cl, and this dye had a blood plasma fluorescence half-life of 195.2 min. Compound 5-Cl at 25 nmol iv had a plasma elimination half-life of 100 min, and 32% of injected dose was excreted through the urine (Figure S18 and Table S1. *Note*: 1-Cl and 5-Cl both may convert the albumin adduct in the blood, but this does not change the fluorescence observed).

CONCLUSIONS

Some important conclusions can be drawn from this study because the key dyes featured (1-Cl, 1-Ph, 5-Cl, and 5-Ph) have complementary properties. MHI-148 derivatives 1 form noncovalent adducts with albumin, but only 1-Cl can form a covalent one. Conversely, QuatCy derivatives 5 do not form noncovalent adducts with albumin, though 5-Cl can form a *covalent* one, but much more slowly than 1-Cl.

Dyes 1-Cl and 5-Cl (which can form covalent adducts) are both retained in tumors, whereas 1-Ph and 5-Ph are not. Both these dyes form noncovalent adducts with albumin, but only the *meso*-chloride derivative forms a covalent one. Consequently, noncovalent binding is insufficient for retention of tumor seeking dyes. It is relevant that 2-Cl (IR-820), which has a *meso*-Cl, localizes in tumors[53,54] but with a TBR< 2.5, i.e. it is a *poor* tumor seeking dye. It is also very slow to form a covalent albumin adduct and this may partially account for its poor tumor uptake and persistence, though other factors like background clearance are probably involved.

Shi and coauthors have hypothesized the cyclohexyl ring of the featured cyanine dyes is responsible for tumor retention, speculating that enhanced rigidity improved uptake via OATPs.[51] Our data contradicts this hypothesis since 1-Ph and 5-Ph have a cyclohexyl ring but do not accumulate or persist in tumors (Figure 6). Moreover, faster *in vivo* clearance of 5-Cl from healthy tissue accounts for the excellent TB contrast observed for this fluorophore after extended times relative to 1-Cl.

Overall, the data presented here is consistent with uptake of tumor seeking dyes more likely being mediated via albumin receptors[55] (known to be overexpressed in cancer cells) than OATPs.[56,57] However, chemical reactivity in pharmacokinetics is rarely clean. While albumin binding accounts for much of the behavior of tumor-seeking dyes, it is unlikely to be the *exclusive* mechanism. Our data does not rule out the possibility that OATPs play a submissive role. The best evidence that this may be so comes from an *in vivo* knockdown experiment reported by Shi and co-workers.[30] Knockdown of OATPs is difficult because there are 11 of them. However, when OATP1B3 was taken out by this method it showed tumor uptake of 1 was reduced by approximately 40% in a PC-3, and by ~25% in $ARCeP_E$, prostate cancer xenograftmodels. To the best of our knowledge, those experiments have never been replicated, but assuming they are general and correct then there can be two interpretations. The first is that OATPs can play a role *in vivo*. The second is that knockdown of OATP1B3 restricts the flow of natural, essential substrates (bile acids, etc.) into the tumor cells and this impacts the ways they take up albumin. Further experimentation, beyond the scope of this study, is required to elaborate on this issue and should not detract from the focus of this work: covalent albumin binding is important for tumor accumulation and persistence. It rationalizes why the *meso*-Cl commonality is tumor seeking.

Cellular uptake experiments in SFM are not indicative of physiological environments because albumin in serum has important effects, but, nevertheless, some inferences can be drawn from those experiments. Formation of noncovalent albumin complexes of dyes 1-Cl and -Ph retards their cellular uptake, but they are both imported; consequently, the *meso*-Cl has no impact on cellular uptake under these conditions (recall, import of 1-Cl and of 1-Ph in the presence of FITC-albumin gave colocalization of the Cy7-and fluorescein-emission). Slower uptake of derivatives 5 than 1 in tissue culture experiments could be associated with failure of the QuatCy derivatives to form noncovalent albumin complexes, and slow formation of a covalent one from 5-Cl (only). This project illustrates that conclusions from cell experiments should not be extrapolated to *in vivo* experiments without qualifiers that

acknowledge the potential impact of the varied dynamic environment inside a mouse relative to the static cell cultures.

In our view, too much emphasis has been placed on the impact of BSP in SFM. In the regard, the evolution of BSP to the status of "probe for OATP receptors" in interesting. In the 1920s, BSP was used as a clinical agent to test clearance from the blood via the liver.[58,59] Subsequently, it was shown that uptake of BSP into rat hepatocytes was via active transport (a saturable, temperature sensitive, ATP-and chloride-dependent mechanism).[60] Later,[61] OATPs ("organic anion binding protein") were discovered, and found to import BSP. Those receptors were also shown to be localized to the surface of hepatocytes.[62] Keppler et al. discovered that BSP is a substrate for some OATPs (e.g., OATP2 not OATP8) and albumin mediated these uptake mechanisms.[63] It appears that after this point BSP gradually became accepted as a *probe* for OATP uptake. It was used to inhibit OATPs in a study of the mechanism of ICG uptake,[64] as a competitor to different anions influxed into cloned cell lines overexpressing OATPs,[40] and, in the past decade, in the context of tumor seeking dyes. However, BSP is also the type of structure classified as a PAIN (Pan Assay INterference compound) in high throughput screening, i.e. a substance likely to bind to many proteins.[65] Consequently, it is unsurprising that BSP may change the cellular uptake properties of albumin complexes of the dyes featured here (and their emission intensities). BSP is *not* an ideal probe for uptake via OATPs in complex cellular media.

Formation of noncovalent and covalent albumin adducts is consistent with a few mechanisms for tumor uptake and persistence. First, noncovalent adduct in serum protects tumor seeking dyes and slows their clearance. Both noncovalent and covalent albumin adducts of 1-Cl might penetrate into cells of the tumor, presumably via albumin receptors overexpressed in cancer cells.[55] Any cyanine dye containing a reactive *meso*-Cl imported into cells will react with albumin or other endogenous thiol nucleophiles like glutathione. Simultaneously, covalent or tight noncovalent adducts of albumin will be drawn to accumulate in tumor tissue by the EPR effect. Indeed, one of the first observations of that effect was for accumulation of labeled-albumin in tumors.[57,66–69] Once tumor seeking dyes are imported into cancer cells comprising the tumor, or trapped in the compressed tumor vasculature via the EPR effect, then they are retained. In fact, Shi has considered EPR as a possible factor that might lead to localization of the dye in tumor tissue.[70] However, EPR is normally associated with large molecules and that work did not directly comment on why a small molecule should do this. Findings presented here "close the circle" on this issue by explaining how tumor-seeking dyes become associated with albumin. Concurrently, these tumor seeking dyes are cleared relatively quickly from healthy tissue (particularly 5-Cl) so imaging *contrast* improves making the fluorescence in the tumor conspicuous.

This work has the following impact on translatability. First, when researchers use tumor-seeking dyes to deliver pharmaceuticals or other imaging agents, they should know that conjugates with a *meso*-chloride will be retained in tumors, but ones with a blocked *meso*-position will not. Second, QuatCy (5-Cl) is preferable to MHI-148 (1-Cl) for imaging based on its exceptionally high tumor-to-background ratio in near-IR fluorescence imaging, and because, uniquely, it is not retained in healthy organs such as the heart, liver, and kidneys. Selectivity of accumulation is also a factor and that issue will be addressed in future work.

MATERIALS AND METHODS

Photophysical Properties.

ICG and IR783 were bought from Ark Pharm and Sigma, respectively. Human serum albumin (HSA), Bovine Serum Albumin (BSA), and BSA labeled with FITC were bought from Sigma-Aldrich. HSA and BSA were stored at −20 °C and fresh 0.5 mM (33 mg in 1 mL) solution was prepared for experiments.

UV Absorbance Experiments.

Compounds 1-Cl, 1-Ph, 5- Cl, 5-Ph, 2-Cl, and ICG were dissolved in PBS (pH 7.4) with HSA and the spectra were taken at different time intervals.

Compounds 1-Cl and 1-Ph (5 μM) were incubated with increasing concentrations of BSP (5, 50, or 250 μM). For blocking experiments, the dyes were either incubated with HSA (5 μM) prior to adding BSP (5, 50, or 250 μM) or increasing concentration of BSP was added to HSA before adding the dyes. The absorbance and fluorescence spectra were determined by Cary-Varian 100 UV−vis NIR spectrophotometer.

UV Absorbance with DMEM.

5 μM 1-Cl, 1-Ph, 5-Cl, and 5-Ph were dissolved FluoroBrite DMEM with or without 10% FBS. The absorbance was determined using Cary-Varian 100 UV−vis NIR spectrophotometer.

Kinetics Experiment.[35]

200 μM of 1-Cl, 1-Ph, 2-Cl, 3-Cl, 4-Cl, 5-Cl, and 5-Ph were dissolved with HSA (500 μM) in PBS pH 7.4. The reaction mixture was kept in an incubator at 37 °C for up to 72 h. The formation of conjugate was observed at 780 nm at different time points using C4 column on Agilent 1200 Infinity II.

Binding Pocket Determination.

Determination of binding pocket of 1-Cl was carried out as reported in the literature.[52,71] Briefly, 5 μM of BSA was preblocked with 50× excess of known binders of pocket I (warfarin), pocket II (ibuprofen), and pocket III (digoxin) for 1 h before adding 5 μM of 1-Cl. The fluorescence was measured using spectrometer.

In Vitro Assays.

MDA-MB-231 and HepG2 cells were grown in Dulbecco's Modified Eagle's medium (DMEM) containing 10% fetal bovine serum (FBS). Cells were grown in an incubator at 37 °C, humidified atmosphere containing 5% CO_2. Cells were grown in T-75 culture flask until 70% confluency before splitting into next passage.

Live Cell Staining.

Uptake of dyes with the MDA-MB-231 and HepG2 cells was measured using Leica SP8 Confocal Microscope. The images were taken at 20×/0.75 water immersed objective. The

NIR dye samples were excited at 670 nm laser (PMT detectors; 716−789 nm) and FITC samples were excited at 490 nm (HyD detectors; 500−589 nm).

BSA-FITC and 1-Cl Colocalization.

Briefly, 50,000 MDA- MB-231 cells were divided into 4 groups: 1. 1-Cl was incubated with BSA-FITC and used immediately. 2. 1-Cl was preincubated with BSA-FITC for 24 h. 3. 1-Cl was incubated with BSA that had Cys^{34} blocked. 4. 1-Ph was incubated with BSA-FITC. Equimolar concentrations of dyes and BSA-FITC were used in each experiment. After 2 h of incubation, the cells were washed twice with PBS and imaged using Leica SP8 Confocal Microscope as mentioned above.

Blocking Experiment.

The cells were divided into 4 groups: 1. control (no serum). 2. with serum. 3. BSP with serum. 4. BSP without serum. Briefly, 50,000 cells were seeded using media containing serum in 4 well chambers (Nunc Lab-Tek) and allowed to adhere overnight. The cells were starved for 4 h in serum free media before the experiment. Group 1 was used as a standard for other groups. Groups 3 and 4 were preblocked for 5 min with 250 μM of BSP with and without serum containing media, respectively. The cells were incubated with 1-Cl, 1-Ph, 2-Cl, 5-Cl, 5-Ph, and ICG for 30 min, washed twice with PBS, and imaged using Leica SP8 Confocal Microscope.

DMOG was added to the chambers 24 h prior to experiment to induce hypoxia in cells. Dyes were added to the chambers for 30 min, washed, and imaged using Leica Microscope.

Cellular uptake of 1-Cl, 1-Ph, 2-Cl, 5-Cl, 5-Ph, and ICG was quantified by using BD FACSAria II. The cells were again divided into 4 groups and treated as mentioned above. After incubation, the cells were washed thrice with PBS, dissociated from the plate using 200 μM of cell dissociation buffer, enzyme free (Thermofisher), and suspended in PBS. The fluorescence of the samples was measured by 633 nm excitation source and 750/45 emission filter.

Cellular uptake of 1-Cl, 1-Ph, 2-Cl, 5-Cl, 5-Ph, and ICG was also quantified using BSA only in the media. MDA-MB-231 cells were seeded on 4 well chamber and starved for 4 h. Dyes were added to the chambers with or without BSA in the solution. Sample without BSA was considered as control and quantified using BD FACSAria II.

Note:

serum free media contains 0% FBS and serum media contains 10%FBS.

Animals and Tumor Models.

Animals were housed in an AAALAC certified facility, and all animal studies were performed under the supervision of MGH IACUC protocols #2016N000136 and #2016N000529. For syngeneic tumor models, 6 wk old (20−30 g) female C57Bl/6 mice were purchased from Taconic Farms and injected subcutaneously in the left flank with E0771 (5×10^6) cells resuspended in 100 μL of PBS. For tumor imaging, 25 nmol of 1-Cl,

1-Ph, 5-Cl, or 5-Ph in 10% BSA was administered intravenously into tumor-bearing mice imaged at different time points (0.5, 1, 2, 4, 24, and 48 h) for up to 48 h.

In Vivo Biodistribution and Clearance.

Mice were anesthetized with ketamine (100 mg/kg) and xylazine (10 mg/kg) before the surgery. A midline incision was performed to open abdominal cavity and 25 nmol of compound 1-Cl, 1-Ph, 5-Cl, or 5-Ph in 10% BSA were injected intravenously into C57Bl/6 mice with subcutaneous triple negative breast tumor and images were taken at 48 h post-administration. Animals were imaged using the in-house built real-time intraoperative NIR fluorescent imaging system. A 760 nm excitation laser source (4 mW/cm^2) was used with white light (400−650 nm; 40,000 lx). Color and NIR fluorescence images were acquired simultaneously with custom software at rates up to 15 Hz over a 15 cm diameter field of view. In the color-NIR merged image, 800 nm fluorescence was pseudocolored red.

Pharmacokinetics and Urinary Excretion.

Animals (25 g CD-1 mice) were injected with 25 nmol of 1-Cl, 1-Ph, 5-Cl, or 5-Ph in saline containing 10% BSA, and the blood sample was collected at the following time points: 0, 10, 30, 60, 120, 180, 240, and 300 min. The samples were centrifuged at 3000 rpm for 20 min to separate plasma and blood cells in capillary tubes. Fluorescence intensities of the plasma at each time point were measured by the NIR imaging system. To determine the urinary excretion rate, the penis of male mice was ligated and 25 nmol of each compound was intravenously administered. The animals were sacrificed 4 h post-injection, and urine was collected, and fluorescence intensity was measured by a UV− vis-NIR spectrophotometer (Ocean Optics).

Quantitative Analysis.

At each time point, the fluorescence (FL) and background (BG) intensity of a region of interest (ROI) over each organ/muscle or tumor/background was quantified using the custom imaging software. The signal-to-background ratio (SBR) was calculated as SBR = target signal/background signal, where a background is surrounding tissue, using ImageJ version 1.52q. At least 3 animals were analyzed at each time point, and statistical analysis was carried out using a one-way ANOVA followed by Tukey's multiple comparisons test. P values less than 0.05 were considered significant: $^{*}P < 0.05$, $^{**}P < 0.01$, and $^{***}P < 0.001$. The experiments were not randomized, and the investigators were not blinded to allocation during experiments and outcome assessment. Results were presented as mean ± s.d. and curve fitting was performed using Microsoft Excel and Prism version7.0a software (GraphPad, San Diego, CA).

Supplementary Material

Refer to Web version on PubMed Central for supplementary material.

ACKNOWLEDGMENTS

We thank DoD BCRP Breakthrough Award (BC141561), CPRIT (RP170144 and RP180875), and The Robert A. Welch Foundation (A-1121), Texas A&M University (RP180875), NIH/NIBIB (R01EB022230) and NSF

(M1603497) for financial support. The NMR instrumentation at Texas A&M University was supported by a grant from the National Science Foundation (DBI-9970232) and the Texas A&M University System. The use Leica SP 8 at Microscopy and Imaging Center facility (MIC) at Texas A&M University and BD Fortessax-20 at College of Medicine Cell Analysis Facility (COM-CAF) is acknowledged. The use of Chemistry Mass Spectrometry Facility is acknowledged.

REFERENCES

(1). van Tellingen O, Yetkin-Arik B, de Gooijer MC, Wesseling P, Wurdinger T, and de Vries HE (2015) Overcoming the blood-brain tumor barrier for effective glioblastoma treatment. Drug Resist. Updates 19, 1–12.

(2). Kushal S, Wang W, Vaikari VP, Kota R, Chen K, Yeh T-S, Jhaveri N, Groshen SL, Olenyuk BZ, Chen TC, et al. (2016) Monoamine oxidase A (MAO A) inhibitors decrease glioma progression. Oncotarget 7, 13842–13853. [PubMed: 26871599]

(3). Lv Q, Yang X, Wang M, Yang J, Qin Z, Kan Q, Zhang H, Wang Y, Wang D, and He Z (2018) Mitochondria-targeted prostate cancer therapy using a near-infrared fluorescence dye-monoamine oxidase A inhibitor conjugate. J. Controlled Release 279, 234–242.

(4). Yang X-G, Mou Y-H, Wang Y-J, Wang J, Li Y-Y, Kong R-H, Ding M, Wang D, and Guo C (2019) Design, Synthesis, and Evaluation of Monoamine Oxidase A Inhibitors-Indocyanine Dyes Conjugates as Targeted Antitumor Agents. Molecules 24, 1400.

(5). Lv Q, Wang D, Yang Z, Yang J, Zhang R, Yang X, Wang M, and Wang Y (2019) Repurposing antitubercular agent isoniazid for treatment of prostate cancer. Biomater. Sci 7, 296–306.

(6). Guan Y, Zhang Y, Xiao L, Li J, Wang J. p., Chordia MD, Liu Z-Q, Chung LWK, Yue W, and Pan D (2017) Improving Therapeutic Potential of Farnesylthiosalicylic Acid: Tumor Specific Delivery via Conjugation with Heptamethine Cyanine Dye. Mol. Pharmaceutics 14, 1–13.

(7). Zhang E, Luo S, Tan X, and Shi C (2014) Mechanistic study of IR-780 dye as a potential tumor targeting and drug delivery agent. Biomaterials 35, 771–778. [PubMed: 24148240]

(8). Wu JB, Shi C, Chu GC-Y, Xu Q, Zhang Y, Li Q, Yu JS, Zhau HE, and Chung LWK (2015) Near-Infrared Fluorescence Heptamethine Carbocyanine Dyes Mediate Imaging and Targeted Drug Delivery for Human Brain Tumor. Biomaterials 67, 1–10. [PubMed: 26197410]

(9). An J, Zhao N, Zhang C, Zhao Y, Tan D, Zhao Y, Bai B, Zhang H, Shi C, An J, et al. (2017) Heptamethine Carbocyanine DZ-1 Dye for Near-Infrared Fluorescence Imaging of Hepatocellular Carcinoma. Oncotarget 8, 56880–56892. [PubMed: 28915639]

(10). Mrdenovic S, Mrdenovic S, Wang R, Yin L, Chu GC-Y, Yin L, Zhau Haiyen E, Chung Leland WK, Zhang Y, Lewis M, et al. (2019) Targeting Burkitt lymphoma with a tumor cell-specific heptamethine carbocyanine-cisplatin conjugate. Cancer 125, 2222. [PubMed: 30840322]

(11). Casi G, and Neri D (2015) Antibody-Drug Conjugates and Small Molecule-Drug Conjugates: Opportunities and Challenges for the Development of Selective Anticancer Cytotoxic Agents. J. Med. Chem 58, 8751–8761. [PubMed: 26079148]

(12). Chari RVJ, Miller ML, and Widdison WC (2014) Antibody-Drug Conjugates: An Emerging Concept in Cancer Therapy. Angew. Chem., Int. Ed 53, 3796–3827.

(13). Srinivasarao M, and Low PS (2017) Ligand-Targeted Drug Delivery. Chem. Rev 117, 12133–12164. [PubMed: 28898067]

(14). Kue CS, Kamkaew A, Burgess K, Kiew LV, Chung LY, and Lee HB (2016) Small Molecules for Active Targeting in Cancer. Med. Res. Rev 36, 494–575. [PubMed: 26992114]

(15). Dagogo-Jack I, and Shaw AT (2018) Tumour heterogeneity and resistance to cancer therapies. Nat. Rev. Clin. Oncol 15, 81–94. [PubMed: 29115304]

(16). Yuan J, Yi X, Yan F, Wang F, Qin W, Wu G, Yang X, Shao C, and Chung LWK (2015) Near-Infrared Fluorescence Imaging of Prostate Cancer Using Heptamethine Carbocyanine Dyes. Mol. Med. Rep 11, 821–828. [PubMed: 25354708]

(17). Zhao N, Zhang C, Zhao Y, Bai B, An J, Zhang H, Shi C, and Wu Jason B (2016) Optical Imaging of Gastric Cancer With Near-Infrared Heptamethine Carbocyanine Fluorescence Dyes. Oncotarget 7, 57277–57289. [PubMed: 27329598]

(18). Yang X, Shao C, Wang R, Chu C-Y, Hu P, Master V, Osunkoya AO, Kim HL, Zhau HE, and Chung LWK (2013) Optical Imaging of Kidney Cancer with Novel Near Infrared Heptamethine Carbocyanine Fluorescent Dyes. J. Urol. (N. Y., NY, U.S.) 189, 702–710.

(19). Yang X, Shi C, Tong R, Qian W, Zhau HE, Wang R, Zhu G, Cheng J, Yang VW, Cheng T, et al. (2010) Near IR Heptamethine Cyanine Dye-Mediated Cancer Imaging. Clin. Cancer Res 16, 2833–2844. [PubMed: 20410058]

(20). Zhang C, Liu T, Su Y, Luo S, Zhu Y, Tan X, Fan S, Zhang L, Zhou Y, Cheng T, et al. (2010) A near-infrared fluorescent heptamethine indocyanine dye with preferential tumor accumulation for in vivo imaging. Biomaterials 31, 6612–6617. [PubMed: 20542559]

(21). Luo S, Yang X, and Shi C (2016) Newly Emerging Theranostic Agents for Simultaneous Cancer targeted Imaging and Therapy. Curr. Med. Chem 23, 483–497. [PubMed: 26695513]

(22). Gao M, Yu F, Lv C, Choo J, and Chen L (2017) Fluorescent chemical probes for accurate tumor diagnosis and targeting therapy. Chem. Soc. Rev 46, 2237–2271. [PubMed: 28319221]

(23). Tan X, Luo S, Wang D, Su Y, Cheng T, and Shi C (2012) A NIR Heptamethine Dye With Intrinsic Cancer Targeting, Imaging and Photosensitizing Properties. Biomaterials 33, 2230–2239. [PubMed: 22182749]

(24). Luo S, Tan X, Qi Q, Guo Q, Ran X, Zhang L, Zhang E, Liang Y, Weng L, Zheng H, et al. (2013) A Multifunctional Heptamethine Near-Infrared Dye for Cancer Theranosis. Biomaterials 34, 2244–2251. [PubMed: 23261220]

(25). Zhang C, Zhao Y, Zhang H, Chen X, Zhao N, Tan D, Zhang H, and Shi C (2017) The Application of Heptamethine Cyanine Dye DZ-1 and Indocyanine Green for Imaging and Targeting in Xenograft Models of Hepatocellular Carcinoma. Int. J. Mol. Sci 18, E1332. [PubMed: 28635650]

(26). Zhang C, Tan X, Tan L, Liu T, Liu D, Zhang L, Fan S, Su Y, Cheng T, Zhou Y, et al. (2011) Labeling stem cells with a near-infrared fluorescent heptamethine dye for noninvasive optical tracking. Cell transplantation 20, 741–51. [PubMed: 21054944]

(27). Tang Q, Liu W, Zhang Q, Huang J, Hu C, Liu Y, Wang Q, Zhou M, Lai W, Sheng F, et al. (2018) Dynamin-related protein 1-mediated mitochondrial fission contributes to IR-783-induced apoptosis in human breast cancer cells. J. Cell. Mol. Med 22, 4474. [PubMed: 29993201]

(28). Thakkar N, Lockhart AC, and Lee W (2015) Role of Organic Anion-Transporting Polypeptides (OATPs) in Cancer Therapy. AAPS J. 17, 535–545. [PubMed: 25735612]

(29). Kotsampasakou E, and Ecker GF (2017) Organic Anion Transporting Polypeptides as Drug Targets, in Transporters as Drug Targets (Sitte HH, Ecker GF, Mannhold R, Buschmann H, and Clausen RP, Eds.) pp 271–324, Wiley -VCH Verlag GmbH & Co. KGaA.

(30). Wu JB, Shao C, Li X, Shi C, Li Q, Hu P, Chen Y-T, Dou X, Sahu D, Li W, et al. (2014) Near-infrared fluorescence imaging of cancer mediated by tumor hypoxia and HIF1α/OATPs signaling axis. Biomaterials 35, 8175–8185. [PubMed: 24957295]

(31). Zhang C, Zhao Y, Zhao N, Tan D, Zhang H, Chen X, Zhang H, An J, Shi C, and Li M (2018) NIRF optical/PET dual-modal imaging of hepatocellular carcinoma using heptamethine carbocyanine dye. Contrast Media Mol. Imaging 2018, 4979746. [PubMed: 29706843]

(32). Xiao L, Zhang Y, Yue W, Xie X, Wang J. p., Chordia MD, Chung LWK, and Pan D (2013) Heptamethine cyanine based 64Cu-PET probe PC-1001 for cancer imaging: Synthesis and in vivo evaluation. Nucl. Med. Biol 40, 351–360. [PubMed: 23375364]

(33). Shi C, Wu JB, Chu GCY, Li Q, Wang R, Zhau HE, Chung LWK, Zhang C, Zhang Y, Pan D, et al. (2014) Heptamethine carbocyanine dye-mediated near-infrared imaging of canine and human cancers through the HIF-1α/OATPs signaling axis. Oncotarget 5, 10114–26. [PubMed: 25361418]

(34). Usama SM, Lin C-M, and Burgess K (2018) On the Mechanisms of Update of Tumor-Seeking Cyanine Dyes. Bioconjugate Chem. 29, 3886–3895.

(35). Lin C-M, Usama SM, and Burgess K (2018) Site-Specific Labeling of Proteins With Near-IR Dyes. Molecules 23, 2900.

(36). Levitt DG, and Levitt MD (2016) Human serum albumin homeostasis: a new look at the roles of synthesis, catabolism, renal and gastrointestinal excretion, and the clinical value of serum albumin measurements. Int. J. Gen. Med 9, 229–255. [PubMed: 27486341]

(37). Canovas C, Bellaye P-S, Moreau M, Romieu A, Denat F, and Goncalves V (2018) Site-specific near-infrared fluorescent labelling of proteins on cysteine residues with meso-chloro-substituted heptamethine cyanine dyes. Org. Biomol. Chem 16, 8831–8836. [PubMed: 30411777]

(38). Thavornpradit S, Usama SM, Shrestha J, Park GK, Choi HS, and Burgess K (2019) QuatCy: A Heptamethine Cyanine Modification With Improved Characteristics. Theranostics 9, 2856–2867. [PubMed: 31244928]

(39). Thavornpradit S, Usama SM, Lin C-M, and Burgess K (2019) Protein Labeling and Albumin Binding Characteristics of The Near-IR Cy7 Fluorophore, QuatCy. Org. Biomol. Chem 17, 7150. [PubMed: 31317168]

(40). Kullak-Ublick G-A, Hagenbuch B, Stieger B, Wolkoff AW, and Meier PJ (1994) Functional characterization of the basolateral rat liver organic anion transporting polypeptide. Hepatology 20, 411–16. [PubMed: 8045503]

(41). Harrison VSR, Carney CE, MacRenaris KW, Waters EA, and Meade TJ (2015) Multimeric Near IR-MR Contrast Agent for Multimodal In Vivo Imaging. J. Am. Chem. Soc 137, 9108–9116. [PubMed: 26083313]

(42). Okamura K, Dummer P, Kopp J, Qiu L, Levi M, Faubel S, and Blaine J (2013) Endocytosis of albumin by podocytes elicits an inflammatory response and induces apoptotic cell death. PLoS One 8, No. e54817. [PubMed: 23382978]

(43). Peters JT (1995) All About Albumin: Biochemistry, Genetics, and Medical Applications.

(44). Gonyar LA, Gray MC, Christianson GJ, Mehrad B, and Hewlett EL (2017) Albumin, in the presence of calcium, elicits a massive increase in extracellular Bordetella adenylate cyclase toxin. Infect. Immun 85, No. e00198. [PubMed: 28396321]

(45). Tian R, Zhu S, Lau J, Chandra S, Niu G, Kiesewetter Dale O, Chen X, Zeng Q, Brooks Bernard R, Ertsey R, et al. (2019) Albumin-chaperoned cyanine dye yields superbright NIR-II fluorophore with enhanced pharmacokinetics. Science Advances 5, No. eaaw0672. [PubMed: 31548981]

(46). Luo S, Zhang E, Su Y, Cheng T, and Shi C (2011) A review of NIR dyes in cancer targeting and imaging. Biomaterials 32, 7127–7138. [PubMed: 21724249]

(47). Kratz F, and Beyer U (1998) Serum proteins as drug carriers of anticancer agents: a review. Drug Delivery 5, 281–299. [PubMed: 19569996]

(48). Baker KJ, and Bradley SE (1966) Binding of sulfobromophthalein (BSP) sodium by plasma albumin–its role in hepatic BSP extraction. J. Clin. Invest 45, 281–287. [PubMed: 5901512]

(49). Wolkoff AW (1987) The role of an albumin receptor in hepatic organic anion uptake: the controversy continues. Hepatology 7, 777–9. [PubMed: 3038726]

(50). Pfaff E, Schwenk M, Burr R, and Remmer H (1975) Molecular aspects of the interaction of bromosulfophthalein with high-affinity binding sites of bovine serum albumin. Mol. Pharmacol 11, 144–152. [PubMed: 1168309]

(51). Tan X, Luo S, Long L, Wang Y, Wang D, Fang S, Ouyang Q, Su Y, Cheng T, and Shi C (2017) Structure-Guided Design and Synthesis of a Mitochondria-Targeting Near-Infrared Fluorophore with Multimodal Therapeutic Activities. Adv. Mater 29, 1704196.

(52). Onoe S, Temma T, Shimizu Y, Ono M, and Saji H (2014) Investigation of cyanine dyes for in vivo optical imaging of altered mitochondrial membrane potential in tumors. Cancer Med. 3, 775− 786. [PubMed: 24737784]

(53). Patel NJ, Manivannan E, Joshi P, Ohulchanskyy TJ, Nani RR, Schnermann MJ, and Pandey RK (2015) Impact of Substituents in Tumor Uptake and Fluorescence Imaging Ability of Near-Infrared Cyanine-like Dyes. Photochem. Photobiol 91, 1219− 1230. [PubMed: 26108696]

(54). Guo Q, Luo S, Qi Q, and Shi C (2013) Preliminary structure-activity relationship study of heptamethine indocyanine dyes for tumor-targeted imaging. J. Innovative Opt. Health Sci 6, 1350003.

(55). Liu Z, and Chen X (2016) Simple bioconjugate chemistry serves great clinical advances: albumin as a versatile platform for diagnosis and precision therapy. Chem. Soc. Rev 45, 1432–1456. [PubMed: 26771036]

(56). Frei E (2011) Albumin binding ligands and albumin conjugate uptake by cancer cells. Diabetol. Metab. Syndr 3, 11. [PubMed: 21676260]

(57). Stehle G, Sinn H, Wunder A, Schrenk HH, Schutt S, Maier-Borst W, and Heene DL (1997) The loading rate determines tumor targeting properties of methotrexate-albumin conjugates in rats. Anti-Cancer Drugs 8, 667–685.

(58). Rosenthal SM (1922) Improved method for using phenoltetrachlorophthalein as a liver function test. J. Pharmacol 19, 385–391.

(59). Rosenthal SM, and White EC (1925) Clinical Application of the Bromsulphalein Test for Hepatic Function. J. Am. Med. Assoc 84, 1112–1114.

(60). Goeser T, Nakata R, Braly LF, Sosiak A, Campbell CG, Dermietzel R, Novikoff PM, Stockert RJ, Burk RD, and Wolkoff AW (1990) The rat hepatocyte plasma membrane organic anion binding protein is immunologically related to the mitochondrial F1 adenosine triphosphatase β-subunit. J. Clin. Invest 86, 220–227. [PubMed: 2142166]

(61). Wolkoff AW, and Chung CT (1980) Identification, purification, and partial characterization of an organic anion binding protein from rat liver cell plasma membrane. J. Clin. Invest 65, 1152−1161. [PubMed: 7364942]

(62). Wolkoff AW, Sosiak A, Greenblatt HC, Van Renswoude J, and Stockert RJ (1985) Immunological studies of an organic anion-binding protein isolated from rat liver cell plasma membrane. J. Clin. Invest 76, 454–459. [PubMed: 3897285]

(63). Cui Y, Konig J, Leier I, Buchholz U, and Keppler D (2001) Hepatic uptake of bilirubin and its conjugates by the human organic anion transporter SLC21A6. J. Biol. Chem 276, 9626–9630. [PubMed: 11134001]

(64). Abels C, Fickweiler S, Weiderer P, Baumler W, Hofstadter F, Landthaler M, and Szeimies R-M (2000) Indocyanine green (ICG) and laser irradiation induce photooxidation. Arch. Dermatol. Res 292, 404–411. [PubMed: 10994775]

(65). Baell JB, and Holloway GA (2010) New Substructure Filters for Removal of Pan Assay Interference Compounds (PAINS) from Screening Libraries and for Their Exclusion in Bioassays. J. Med. Chem 53, 2719–2740. [PubMed: 20131845]

(66). Noguchi Y, Wu J, Duncan R, Strohalm J, Ulbrich K, Akaike T, and Maeda H (1998) Early phase tumor accumulation of macromolecules: a great difference in clearance rate between tumor and normal tissues. Jpn. J. Cancer Res 89, 307–314. [PubMed: 9600125]

(67). Torchilin Vladimir P (2010) Passive and active drug targeting: drug delivery to tumors as an example. Handb. Exp. Pharmacol 197, 3–53.

(68). Heneweer C, Holland JP, Divilov V, Carlin S, and Lewis JS (2011) Magnitude of enhanced permeability and retention effect in tumors with different phenotypes: 89Zr-albumin as a model system. J. Nucl. Med 52, 625–633. [PubMed: 21421727]

(69). Lammers T, Kiessling F, Hennink WE, and Storm G (2012) Drug targeting to tumors: Principles, pitfalls and (pre-) clinical progress. J. Controlled Release 161, 175–187.

(70). Shi C, Wu Jason B, and Pan D (2016) Review on near-infrared heptamethine cyanine dyes as theranostic agents for tumor imaging, targeting, and photodynamic therapy. J. Biomed. Opt 21, 50901. [PubMed: 27165449]

(71). Poor M, Kunsagi-Mate S, Czibulya Z, Li Y, Peles-Lemli B, Petrik J, Vladimir-Knezevic S, and Koszegi T (2013) Fluorescence spectroscopic investigation of competitive interactions between ochratoxin A and 13 drug molecules for binding to human serum albumin. Luminescence 28, 726–733. [PubMed: 22987806]

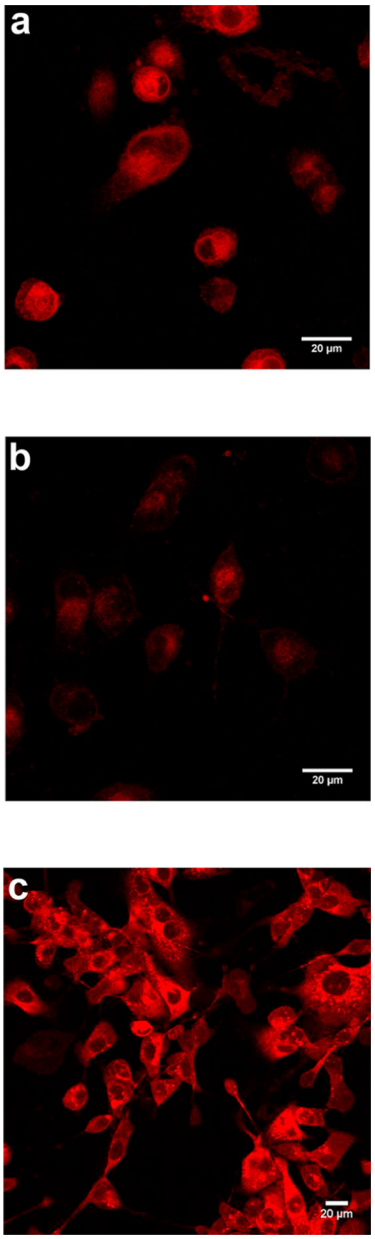

Figure 1.

a, MDA-MB-231 cells incubated with 1-Ph (20 μM) SFM; b, same experiment but preblocked by incubating with 250 μM BSP for 5 min; c same as a, but cells pretreated with 1 mM DMOG to induce hypoxia. Figure S1 shows data from identical experiments but using 1-Cl. Throughout, images were taken by Leica Confocal Microscope at 20×/0.75 NA.

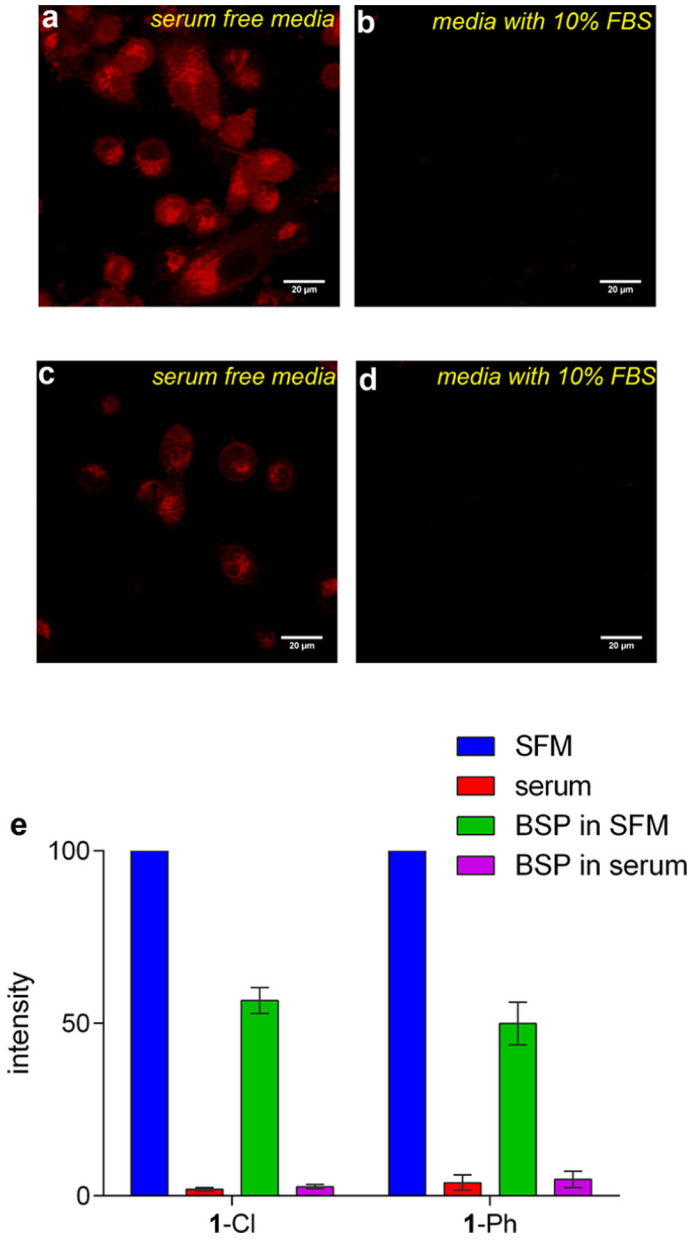

Figure 2.

1-Cl (20 μM) in a, serum free media; b, media with 10% FBS; c, 250 μM BSP serum free; and d, 250 μMBSP with media containing 10%FBS; and e, quantification of the data in a−d by FACS.

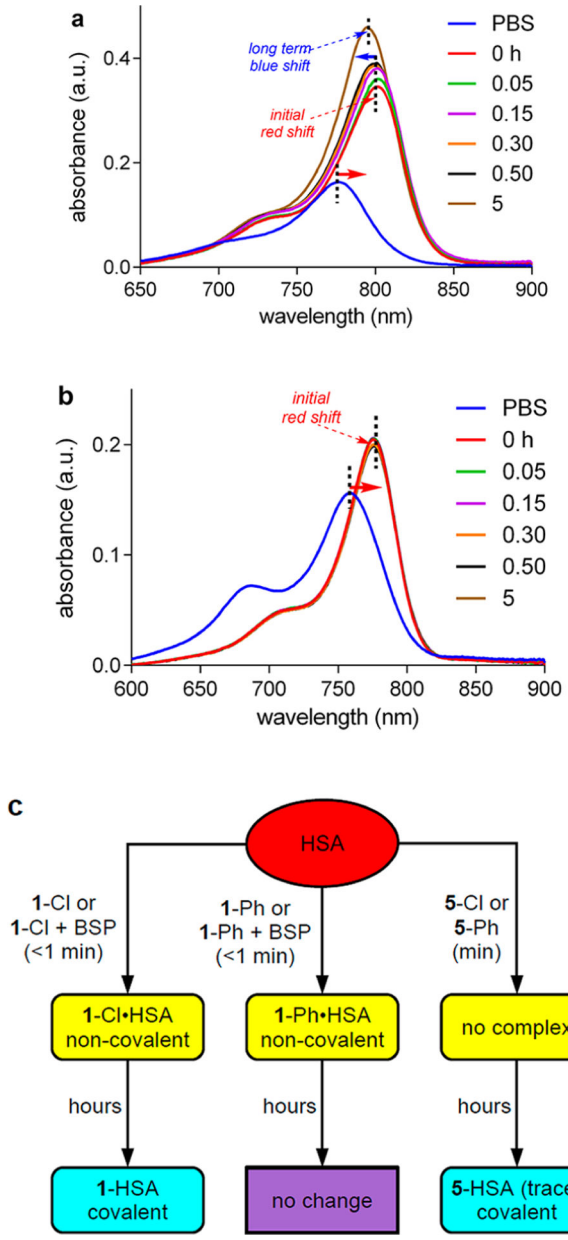

Figure 3.

Interaction of a, 1-Cl; and b, 1-Ph (1 μM) with HSA (50 μM) at pH 7.4 in PBS buffer at 37 °C observed via UV−vis spectroscopy. c, Summary of key UV experiments for albumin interactions with 1, 5, and BSP.

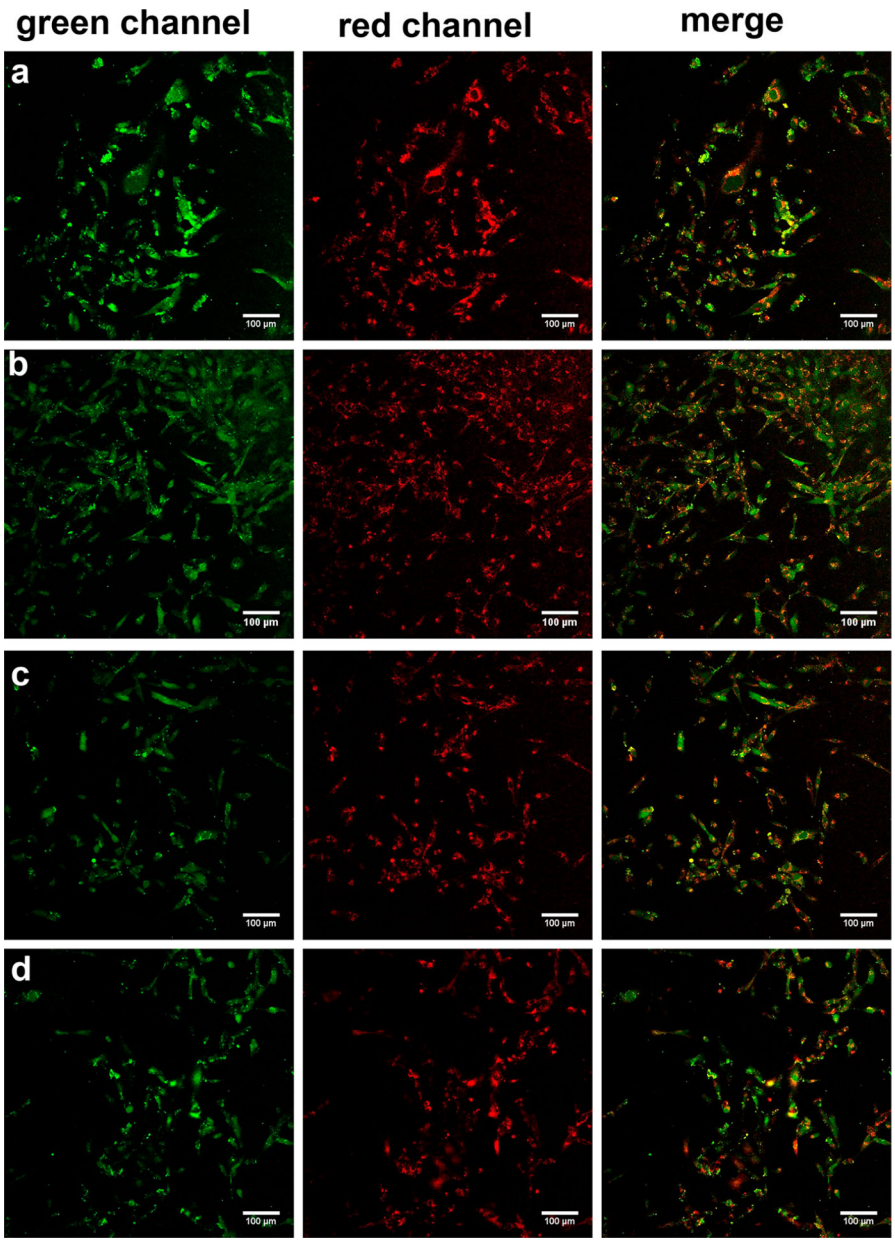

Figure 4.

MDA-MB-231 cells incubated with the following. a, 1-Cl (10 μM throughout) and ~1 equiv BSA-FITC (mixed then used as a noncovalent adduct, i.e., before a covalent adduct could form). b, 1-Cl preincubated with ~1 equiv of BSA-FITC for 24 h to form covalent adduct. c, 1-Cl with BSA-FITC preincubated with 6-maleimidohexanoic acid for 24 h to block Cys.[34] d, 1-Ph (10 μM) and ~1 equiv BSA-FITC. Throughout the incubation conditions were at 37 °C and 5% CO_2 in 20 min unless otherwise indicated. Images at 20× magnification.

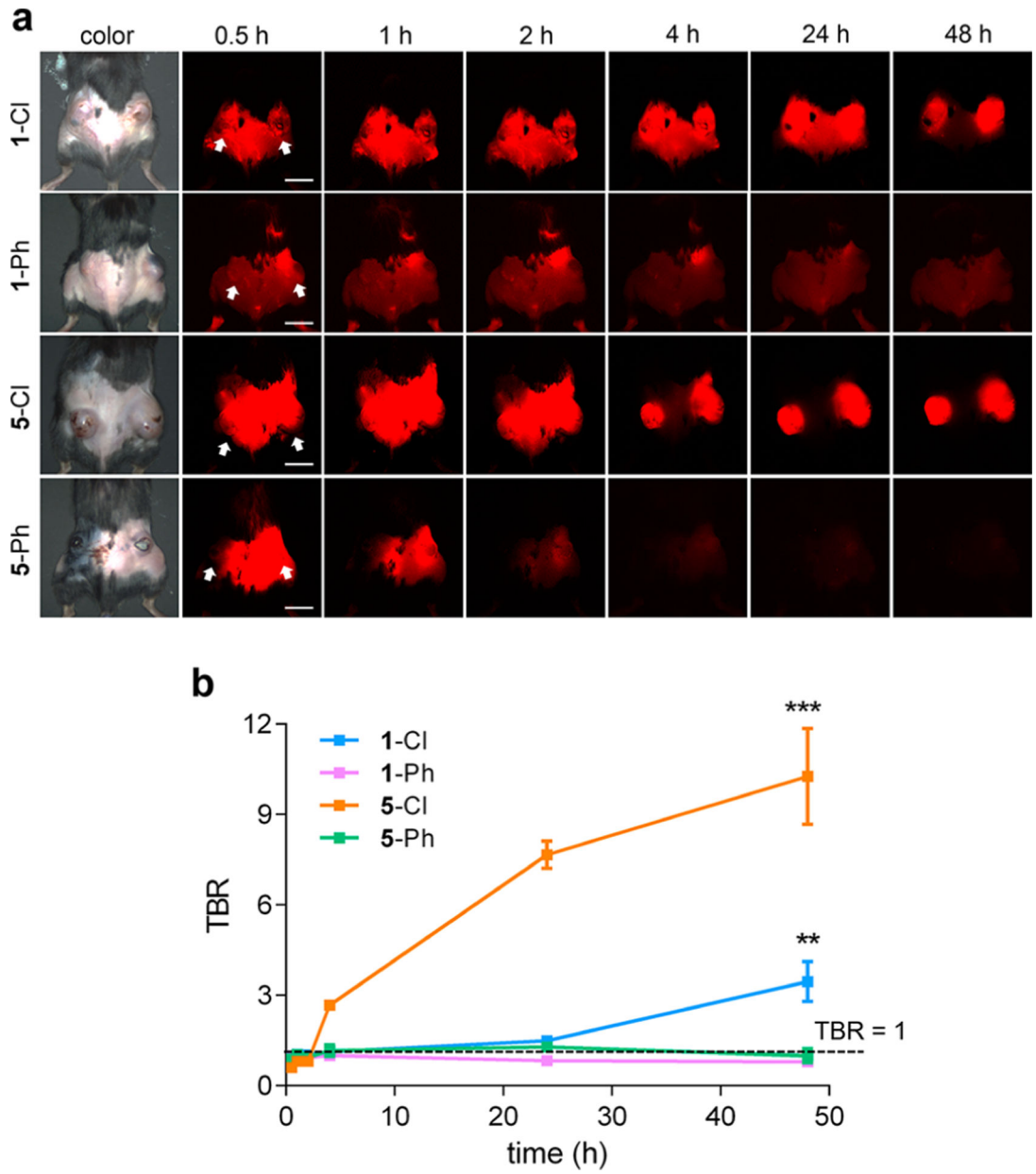

Figure 5.

a, Tumor localization of 1-Cl, 1-Ph, 5-Cl, and 5-Ph. b, Time course of tumor to background ratios (TBRs). Arrows indicate tumors. Scale bars = 1 cm. *$P < 0.05$, **$P < 0.01$, and ***$P < 0.001$.

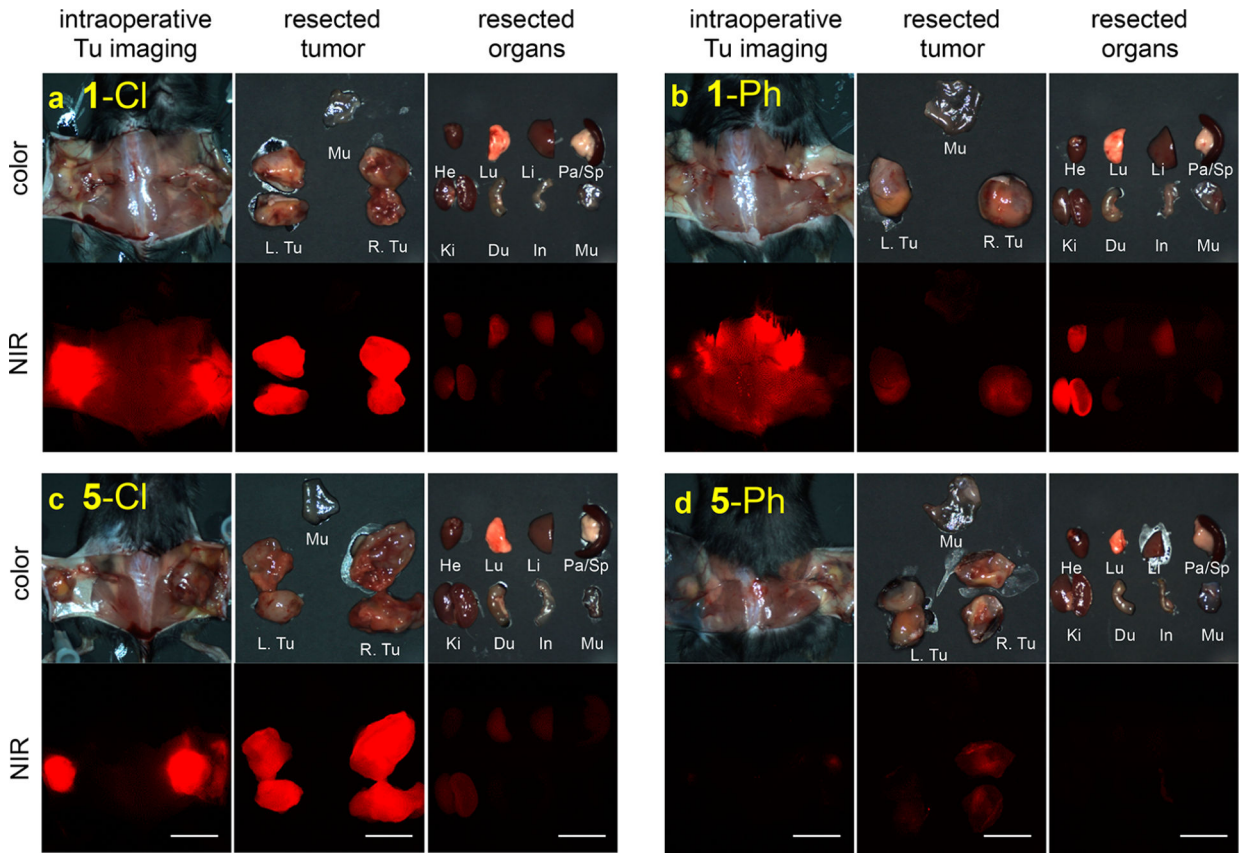

Figure 6.

Intraoperative imaging and biodistribution after 48 h for 25 nmol: a, 1-Cl; b, 1-Ph; c, 5-Cl; and, d, 5-Ph, in C57Bl/6 mice with subcutaneous triple negative breast tumor (E0771). Scale bars = 1 cm. He, heart; Lu, lung; Li, liver; Pa, pancreas; Sp, spleen; K_i, kidney, Du;duodenum; In, intestine; Mu, muscle; and Tu, tumor.